

# 1 **Sensory population activity reveals confidence computations 2 in the primate visual system**

3 **Zoe M. Boundy-Singer<sup>1,2</sup>, Corey M. Ziembra<sup>1,3</sup>, Robbe L. T. Goris<sup>1\*</sup>**

4 <sup>1</sup> Center for Perceptual Systems, University of Texas at Austin, Austin, Texas, 78712, USA. <sup>2</sup> Current address: McGovern In-  
5 stitute for Brain Research, Massachusetts Institute of Technology, Cambridge, MD, 02139, USA. <sup>3</sup> Current address: Laboratory  
6 of Sensorimotor Research, National Eye Institute, National Institutes of Health, Bethesda, MD, 20892, USA. \*Correspondence:  
7 robbe.goris@utexas.edu.

8 **Perception is fallible<sup>1-3</sup>. Humans know this<sup>4-6</sup>, and so do some non-human animals like macaque monkeys<sup>7-14</sup>. When**  
9 **monkeys report more confidence in a perceptual decision, that decision is more likely to be correct. It is not known how**  
10 **neural circuits in the primate brain assess the quality of perceptual decisions. Here, we test two hypotheses. First, that**  
11 **decision confidence is related to the structure of population activity in sensory cortex. And second, that this relation dif-**  
12 **fers from the one between sensory activity and decision content. We trained macaque monkeys to judge the orientation**  
13 **of ambiguous stimuli and additionally report their confidence in these judgments. We recorded population activity in**  
14 **the primary visual cortex and used decoders to expose the relationship between this activity and the choice-confidence**  
15 **reports. Our analysis validated both hypotheses and suggests that perceptual decisions arise from a neural computation**  
16 **downstream of visual cortex that estimates the most likely interpretation of a sensory response, while decision confidence**  
17 **instead reflects a computation that evaluates whether this sensory response will produce a reliable decision. Our work**  
18 **establishes a direct link between neural population activity in sensory cortex and the metacognitive ability to introspect**  
19 **about the quality of perceptual decisions.**

20 **Keywords||** neural coding, visual cortex, sensory uncertainty, population representation, metacognition

## 21 **Introduction**

22 Perceptual interpretations of the environment are automatically accompanied by a sense of confidence in this interpretation. For  
23 example, when soccer fans in a football stadium see a striker score a goal, they may hold their breath and ask other fans whether  
24 the ball really went in. Judging the trajectory of fast moving objects is difficult, and we know this. The ‘metacognitive’ ability  
25 to evaluate the quality of perceptual interpretations helps us to plan future actions<sup>15</sup>, learn from mistakes<sup>16,17</sup>, and optimize  
26 group decision-making<sup>18</sup>. How does the brain assess the quality of perceptual decisions? A prominent hypothesis is that early  
27 areas in sensory cortex provide raw sensory measurements which are used by downstream circuits in association cortex to  
28 guide perceptual decisions<sup>19-22</sup> and assign confidence in these decisions<sup>7,10,12,13</sup>. It follows that there may exist a systematic  
29 relationship between neural population activity in sensory cortex and confidence in perceptual decisions. Here, we set out to  
30 test this hypothesis and document the basic characteristics of this relationship.

31 To examine the relationship between sensory activity and confidence, we developed a task that invites subjects to jointly  
32 report a perceptual decision and their confidence in this decision (also see the work by M. Vivar-Lazo & C.R. Fetsch, *SFN*  
33 *Abstract*, Population dynamics in areas MT and LIP during concurrent deliberation toward a choice and confidence report,  
34 212.11, 2022). We trained two macaque monkeys (F and Z) to judge whether a visual stimulus presented near the central  
35 visual field was oriented clockwise or counterclockwise from vertical. The monkeys communicated their judgment with a  
36 saccade to one of four choice targets, organized in a rectangular pattern around the fixation mark (Fig. 1a). Horizontal saccade  
37 direction indicated the perceptual judgement, vertical saccade direction indicated the confidence in the decision. Choices were  
38 rewarded in a manner that incentivizes observers to introspect about decision quality on a trial-by-trial basis. Specifically,  
39 high confidence judgements resulted in a larger immediate reward when correct, but in a loss of potential future reward when  
40 incorrect (see Methods). While the animals performed this task, we recorded extracellular responses from neural populations in  
41 primary visual cortex (V1), the first sensory area in the primate visual system where individual neurons signal the task relevant  
42 feature, stimulus orientation<sup>23</sup>.

43 We found that confidence in perceptual decisions can be predicted from V1 population activity. The relationship between  
44 sensory activity and decision confidence appears as strong as the relationship between sensory activity and decision content.  
45 This assessment is based on the analysis of one hidden-layer neural networks trained to either predict the perceptual choice or the  
46 confidence report from V1 population activity. In both cases, the networks captured behavioral effects of stimulus manipulations  
47 (variations in stimulus orientation and stimulus contrast) as well as behavioral variability under repeated presentations of the  
48 same stimulus. As predicted by theoretical models of perceptual confidence, the relation between sensory activity and decision

49 confidence fundamentally differs from the one between sensory activity and decision content. It involves an additional non-  
50 linearity and consideration of sensory uncertainty. Together, these results reveal how an essential metacognitive ability arises  
51 from downstream transformations of neural population activity in sensory cortex.

## 52 Results

### 53 Behavior and computational hypothesis

54 Both monkeys learned to report confidence in a fine orientation discrimination task. Their perceptual choices lawfully depended  
55 on stimulus orientation, and they made few errors in the easiest stimulus conditions (monkey F =  $\pm$  18.2 degrees, median  
56 performance, 100 % correct; monkey Z =  $\pm$  15.0 degrees, median performance, 100 % correct). Consider the choice behavior  
57 for an example recording session. Choices reported with high confidence are shown in green, choices reported with low  
58 confidence in red, and symbol size is proportional to the number of trials (Fig. 1b). As is evident from the raw data, for every  
59 stimulus condition, high confidence choices tended to be more accurate than low confidence choices (Fig. 1b, green vs red  
60 symbols). As a consequence, high confidence choices exhibited a steeper overall relationship with stimulus orientation (Fig.  
61 1b, green vs red curve). We quantified this effect by estimating the slope of both psychometric functions and computing the  
62 slope ratio (Methods). For the vast majority of recording sessions, high confidence choices were associated with a steeper  
63 psychometric function than low confidence choices (monkey F: median slope ratio = 0.42,  $P < 0.001$ , Wilcoxon signed rank  
64 test against 1; monkey Z = 0.40,  $P < 0.001$ ; Fig. 1c). This effect mirrored the choice behavior of a group of human subjects,  
65 naive to the purpose of our study, who performed a similar orientation discrimination task ( $N = 19$ , median slope ratio = 0.27,  $P$   
66  $< 0.001$ ; Fig. 1c; Methods). These results suggest that the monkeys introspected about the quality of each perceptual decision  
67 and relied on a confidence assignment process that is qualitatively similar to the one used by humans (see Supp. Fig. 1 for  
68 further comparison).

69 We wondered whether the monkeys' ability to assess the quality of perceptual decisions quantitatively resembles that of humans.  
70 The statistic we have considered thus far is inadequate to answer this question. The association between confidence and the  
71 slope of the psychometric function is a robust signature of sensible confidence assessments, but the slope ratio does not only  
72 depend on the quality of confidence assessments. It also depends on the subject's perceptual sensitivity and their proclivity  
73 to report high confidence<sup>24</sup>. We therefore quantified the quality of the confidence reports by computing each subject's meta-  
74 uncertainty (Methods). Meta-uncertainty is a statistic that expresses how well a decision maker can discriminate reliable from  
75 unreliable choices, regardless of their level of perceptual sensitivity and response biases<sup>24</sup>. Surprisingly, we found that the  
76 monkeys outperformed the human subjects during this group's first visit to the lab (humans performed 1,100 trials in block 1,  
77 median  $\sigma_m = 1.56$ , median  $\sigma_m$  monkeys = 0.47,  $P < 0.001$ , Wilcoxon rank sum test; Fig. 1d, Humans 1 vs monkeys). We  
78 reasoned that task experience was the likely driver of this effect. To test this, we asked the human subjects to perform the  
79 experiment two more times. Reassuringly, they eventually caught up with the monkeys (median  $\sigma_m$  humans in block 3 = 0.57,  
80 median  $\sigma_m$  monkeys = 0.47,  $P = 0.58$ ; Fig. 1d). We conclude that our animal paradigm invites high-quality metacognitive  
81 behavior.

82 What is the nature of the confidence assignment process that underlies this metacognitive capacity? Previous work has shown  
83 that choice-confidence data in tasks like ours are often well captured by a hierarchical process model in which confidence  
84 reflects an observer's estimate of the reliability of their decision<sup>24–27</sup>. In these models, a stimulus gives rise to a noisy, one-  
85 dimensional decision variable (for example, a perceptual orientation estimate). Comparison of this decision variable with a  
86 fixed criterion yields a perceptual decision ('clockwise' or 'counterclockwise'; Fig. 1e, top). The reliability of this decision  
87 is revealed by computing the distance between the decision variable and the decision criterion, and normalizing this distance  
88 by an estimate of the uncertainty of the decision variable (Fig. 1e, middle). Comparison of this decision reliability estimate  
89 with a fixed confidence criterion yields a confidence report ('confident' or 'not confident'; Fig. 1e, bottom). The quality of the  
90 confidence reports is limited by a subject's uncertainty about the uncertainty of the decision variable ('meta-uncertainty')<sup>24</sup>,  
91 or by an analogous noise term, depending on the specific model variant<sup>25,26</sup>. As can be seen for an example dataset, this  
92 computational framework captures how the monkey's tendency to choose the 'confident' response option jointly depends on  
93 stimulus orientation and stimulus contrast (Fig. 1f, Supp. Fig. 1d,e).

94 Decision-making areas downstream of sensory cortex do not get one-dimensional perceptual estimates as input, but high-  
95 dimensional population responses. They implement operations akin to these idealized model computations by mapping this  
96 population activity onto the available choice options. To gain an intuition for these mapping rules, consider a pair of hypothetical  
97 V1 neurons whose responses selectively depend on stimulus orientation and stimulus contrast (Fig. 1g). One of these neurons  
98 prefers orientations smaller than 0 degrees, while the other one on average responds more vigorously to orientations larger than  
99 0 degrees. Thus, their joint activity pattern contains information about stimulus orientation, regardless of stimulus contrast.  
100 Specifically, when neuron 2 is more active than neuron 1, the stimulus is more likely to be oriented clockwise from vertical

101 and vice versa (Fig. 1h, left). The mapping rule used by a downstream decision-making circuit can thus be understood as  
102 projecting the population activity onto a one-dimensional axis perpendicular to a linear hyperplane that separates clockwise  
103 from counterclockwise response patterns (Fig. 1h, middle). The resulting decisions will not be flawless – due to neural  
104 response variability, there is considerable overlap between both response distributions, making errors inevitable. Crucially, the  
105 population response also contains information about the probability of such an error. The closer the population activity is to the  
106 hyperplane, the more probable an error. This effect is amplified for activity patterns that reside close to the bottom left corner  
107 of this state space. This part of the space is visited when the stimulus-drive is weak, for example because stimulus contrast is  
108 low or stimulus size is small. Here, response patterns are dominated by spontaneous activity, resulting in high levels of sensory  
109 uncertainty<sup>28–31</sup> and many incorrect decisions (Fig. 1h, right). These geometrical considerations yield two testable predictions.  
110 First, that decision confidence is related to the structure of population activity in sensory cortex. And second, that this relation  
111 differs from the one between sensory activity and decision content.

## 112 Predicting perceptual decision confidence from V1 activity

113 While the animals performed the perceptual confidence task, we used multilaminar electrode arrays to record population activity  
114 from ensembles of V1 units whose receptive fields overlapped with the stimulus location (Methods). Populations ranged in  
115 size from 8 to 46 units (median = 15 units). Consider the activity of three simultaneously recorded units. Stimulus onset  
116 elicited a strong transient response, followed by a weaker sustained response (Fig. 2a). Some units were better driven by  
117 counterclockwise orientations (Fig. 2a, top), some by clockwise orientations (Fig. 2a, bottom), and some did not differentiate  
118 between these stimulus conditions (Fig. 2a, middle). We first asked whether the observed populations could in principle  
119 provide the sensory signals to support the perceptual task. To this end, we trained linear *stimulus decoders* to discriminate  
120 between clockwise and counterclockwise stimuli and tested them on non-ambiguous hold-out trials (Methods; Fig. 2b). We  
121 found that each recorded population could support the perceptual task above chance level (neural performance ranged from 57.4  
122 to 96.9% correct, median = 69.2%). These decoders have only been provided with neural population responses and stimulus  
123 labels ('clockwise' or 'counterclockwise'). Yet it is natural to ask whether they can offer some insight into the monkeys'  
124 behavior. We compared the stimulus decoders' choices with the animals' reports on a trial-by-trial basis and found that the  
125 fraction of correctly predicted perceptual decisions exceeded the number expected by chance (median difference = 6.3%,  $P$   
126 < 0.001, Wilcoxon signed rank test; Fig. 2b). Both variables exhibited a clear relationship; the better the neural populations  
127 could support the perceptual task, the better the stimulus decoder predicted perceptual decisions (Pearson correlation:  $r$  =  
128 0.79,  $P$  < 0.001, Fig. 2b). This finding is consistent with the hypothesis that decision-making circuits downstream of visual  
129 cortex estimate the most likely interpretation of a sensory response, just like these stimulus decoders do. We also compared the  
130 stimulus decoders' output with the animals' confidence reports and found them to be unrelated (median Pearson correlation =  
131 -0.03,  $P$  = 0.16; Fig. 2c). This result is not surprising. It simply confirms that in our task, the relationship between sensory  
132 activity and decision content cannot account for decision confidence.

133 To expose the relationship between sensory population activity and decision confidence, we trained *confidence decoders* to  
134 discriminate between trials in which monkeys reported choices with either high or low confidence. For this analysis, we  
135 considered both linear and non-linear decoders (specifically, one-hidden layer neural networks; Methods). Linear decoders can  
136 slice a high-dimensional space in various ways (Fig. 2d, left), but none of the possible variations fully captures the hypothesized  
137 confidence mapping rule (Fig. 1h, right). Non-linear decoders can implement more complex input-output relations (Fig.  
138 2d, right), making them better suited to test the hypothesis. Importantly, this additional complexity is not guaranteed to be  
139 beneficial. This will only be the case if the brain's mapping rule requires the complexity (compare Fig. 1h, middle and right).  
140 To connect this concept to our data, we first compared linear and non-linear *choice decoders* trained to predict perceptual  
141 decisions (Methods). We orthogonalized the neural choice and confidence subspaces by curating the decoders' training sets  
142 such that the animals' perceptual choice contained no information about their confidence report and vice versa (Methods;  
143 Supp. Fig. 2a). As expected, linear and non-linear choice decoders performed similarly well, suggesting that a linear mapping  
144 rule suffices to relate sensory population activity to perceptual decisions (median performance linear choice decoder = 66.8%  
145 correctly predicted choices; non-linear choice decoder = 68.8%, median difference = -0.7%,  $P$  = 0.34, Wilcoxon signed rank  
146 test; Fig. 2e). We then performed the same comparative analysis on the confidence reports and obtained a different result.  
147 The nonlinear confidence decoders consistently outperformed their linear counterparts in predicting confidence (median linear  
148 confidence decoder = 61.8% correctly predicted confidence reports; non-linear confidence decoder = 65.6%, median difference  
149 = 4.0%,  $P$  < 0.001; Fig. 2f). In general, confidence reports could be predicted about as well as perceptual decisions (median  
150 performance difference between non-linear choice and confidence decoders = 3.5%,  $P$  = 0.19). Together, these results confirm  
151 that perceptual decision confidence is related to the structure of population activity in sensory cortex, and that this relationship  
152 is more complex than the relation between this activity and decision content.

## 153 Interrogating the confidence decoder

154 We seek to understand how sensory population activity informs confidence in perceptual decisions. So far, our analysis suggests  
155 that non-linear decoders trained to predict behavioral choice-confidence reports from neural population activity are a powerful  
156 tool in this endeavour. Of course, this is only true to the extent that the mapping relation learned by the decoders resembles  
157 the one used by the brain. This need not be the case. Clearly, the confidence decoders are imperfect predictors of the animals'  
158 behavior. It is possible that their success is based on exploiting idiosyncratic relationships between neural responses and  
159 confidence reports that are distinct from the brain's confidence computation<sup>32</sup>. If this were the case, the confidence decoders'  
160 output should not exhibit the key signature of sensible confidence assignments, nor should they be able to generalize to new  
161 testing conditions. We investigated both issues. We first computed the slope of the psychometric function, conditioned on  
162 the confidence decoder's output (Methods; Fig. 3a). Higher confidence outputs were associated with a steeper psychometric  
163 function (median slope ratio = 0.88,  $P = 0.02$ , Wilcoxon signed rank test, Fig. 3b). This pattern recapitulates a key feature of  
164 the animals' behavior and implies that the confidence decoder's outputs are sensible. The confidence decoder recognizes which  
165 neural responses are more likely to result in a reliable perceptual decision.

166 If the mapping rule learned by the confidence decoder resembles the one used by the brain, it should transfer to more challenging  
167 testing conditions, such as input patterns it has not been exposed to during training. To test this, we probed the confidence  
168 decoders with synthetic patterns of neural activity. We designed these patterns such that they would expose the 'pure' effects  
169 of stimulus orientation and stimulus contrast on decision confidence. Specifically, for every stimulus orientation, we created a  
170 synthetic pattern by computing the trial-averaged population response, thus removing the effects of neural response variability  
171 (Methods). We captured the effects of stimulus contrast by changing the gain of the synthetic neural responses<sup>33–35</sup>. Here, we  
172 went far outside the range of our experimental stimulus manipulation to create out-of-distribution inputs (Methods). Consider  
173 the decoder's confidence-outputs for an example recording session. More extreme orientations are always associated with more  
174 high confidence outputs, regardless of the level of response gain (Fig. 3c). Additionally, higher levels of response gain are  
175 always associated with more high confidence outputs, regardless of the stimulus orientation (Fig. 3c). These effects were  
176 evident across datasets (median difference in predicted proportion high confidence outputs for more vs less extreme stimulus  
177 orientations = 15%,  $P < 0.001$ ; median difference for a response gain of 0.5 and 2 = 38%,  $P < 0.001$ ; Wilcoxon signed rank  
178 test; Fig. 3d). Thus, the decoder's confidence output jointly depends on stimulus orientation and stimulus contrast, thereby  
179 recapitulating the second key feature of the animals' behavior (Supp. Fig. 1e). Moreover, the mapping rule learned by the  
180 decoder generalizes to new testing conditions. We conclude that the confidence decoder evaluates neural activity in a sensible  
181 and robust manner.

## 182 Relationship between choice and confidence computations

183 Our analysis of neural activity was inspired by a computational framework in which confidence reflects an observer's estimate  
184 of the reliability of their decision<sup>24–26</sup>. In this framework, the computations that form a decision are distinct from the ones that  
185 assign confidence in these decisions. However, there is a direct relationship between the latent variables that underlie the overt  
186 perceptual choices and confidence reports. Specifically, more extreme decision variable values will yield higher confidence  
187 variable values (Fig. 1e, middle). The decoders we trained on neural data use a latent variable to predict behavioral choice-  
188 confidence reports (Methods). We wondered whether these latent variables would be related as predicted by the computational  
189 framework. If this were the case, it would provide direct evidence for the notion that the brain's confidence computation  
190 evaluates the quality of the sensory evidence that informed the decision.

191 Consider the neurally decoded decision variable for an example recording session. There are three important effects. The  
192 decision variable varies linearly with stimulus orientation (Fig. 4a). The slope of this relationship depends on stimulus contrast  
193 (Fig. 4a, left vs right panel). And trials that culminate in a "clockwise decision" are associated with a higher decision variable  
194 value (Fig. 4a, yellow vs blue). These effects were present in most of our datasets (median slope for high contrast stimuli =  
195 0.064,  $P < 0.001$ ; median reduction in slope for low contrast stimuli = 0.02,  $P = 0.04$ ; median change in offset with perceptual  
196 choice = 0.22,  $P < 0.001$ , Wilcoxon signed rank test; Fig. 4b). The neurally decoded confidence variable exhibits a different  
197 structure. It varies parabolically with stimulus orientation (Fig. 4c). The width and offset of the parabola depend on stimulus  
198 contrast (Fig. 4c). And trials that culminate in a "high confidence" report are associated with a higher confidence variable value  
199 (Fig. 4c). Again, these effects were present in most of our datasets (median quadratic coefficient for high contrast stimuli =  
200 0.002,  $P < 0.001$ ; median change in this coefficient for low contrast stimuli = 0.001,  $P = 0.005$ ; median change in offset for low  
201 contrast stimuli = 0.15,  $P < 0.001$ ; median change in offset with confidence report = 0.11,  $P < 0.001$  Wilcoxon signed rank test;  
202 Fig. 4d). To compare the strength of the association of both decision and confidence latent variables with the overt behavior, we  
203 computed their ability to discriminate behavior in the absence of stimulus variation (Methods). A discriminability value of 50%  
204 corresponds to chance performance, while 100% means that the behavior can be perfectly predicted from the latent variable.  
205 For both perceptual choices and confidence reports, we found a modest association (median decision variable discriminability

206 = 54%,  $P < 0.001$ ; median confidence variable discriminability = 56%,  $P < 0.001$ , Wilcoxon signed rank test; Fig. 4b,d). This  
207 association tended to be stronger for populations that contained more stimulus information (Supp. Fig. 2b). Thus, the decoders'  
208 latent variables provide insight into the neural processes underlying the overt choice-confidence reports.

209 Plotting the confidence variable against the decision variable for all trials of an example recording session reveals a U-shaped  
210 relationship, consistent with the proposed confidence computation (Fig. 4e, left). If this relationship arises from this computa-  
211 tion, it should leave a signature even within the same stimulus conditions. Specifically, trials that yield a more extreme decision  
212 variable value should result in a higher value of the confidence variable. To test this prediction, we computed the median of  
213 the decision variable for every stimulus condition and computed the average of the confidence variable separately for trials  
214 above and below the median. As can be seen for an example recording session, more extreme decision variable values were  
215 systematically associated with higher levels of confidence (Fig. 4e, right). This effect was evident across all datasets, for both  
216 monkeys (median difference in confidence variable: monkey F = 0.06,  $P < 0.001$ , monkey Z = 0.11,  $P < 0.001$ ; Fig. 4f). Our  
217 analysis ensured that choice and confidence signals occupied orthogonal neural dimensions (Methods). We therefore conclude  
218 that the brain's confidence computation evaluates the same sensory population activity that informed the decision.

## 219 Discussion

220 In this study, we investigated neural population activity in V1 during a perceptual confidence task. We sought to understand the  
221 brain's confidence assignment process. This process underlies the metacognitive ability to evaluate the quality of perceptual  
222 interpretations. We suggest that confidence arises from a nonlinear transformation of the same sensory signals that inform  
223 perceptual decisions. When the sensory population response is strong and unambiguous, this transformation results in high  
224 decision confidence (Fig. 1h, green zone). Conversely, when the sensory population response is weak or ambiguous, it results  
225 in low levels of confidence (Fig. 1h, red zone). Our proposal is supported by three distinct observations. First, nonlinear  
226 decoders of V1 population activity can predict monkeys' confidence in perceptual orientation judgments (Fig. 2f), establishing  
227 a direct link between the structure of sensory activity and decision confidence. Second, these decoders yield sensible and robust  
228 confidence outputs when presented with synthetic patterns of neural activity (Fig. 3), suggesting they capture the essence of the  
229 brain's confidence computation. Third, trials that yield stronger and less ambiguous V1 responses as evidenced by a neurally  
230 decoded decision variable also result in higher levels of neurally decoded confidence (Fig. 4).

231 Our experimental paradigm enabled us to compare choice and confidence decoders trained on the same neural responses. We  
232 found that the relationship between sensory activity and decision confidence is as strong as the relationship between sensory  
233 activity and perceptual choice (Fig. 2e,f and Fig. 4b,d). However, we suggest that there is a fundamental difference between  
234 both relationships. Perceptual choices arise from a neural computation downstream of sensory cortex that identifies the most  
235 likely interpretation of the sensory response; decision confidence instead arises from a computation that evaluates whether this  
236 sensory response will produce a reliable decision (Fig. 1e). Because these computations are distinct, they can manifest as  
237 mapping rules of sensory population activity that occupy orthogonal neural subspaces (Fig. 1h). Previous work offers indirect  
238 support for these ideas. Specifically, micro-stimulating sensory neurons in a post-decision wagering task altered monkeys' opt-  
239 out choice behavior as if they experienced a change in the sensory signal<sup>10</sup>. These results suggest that the same sensory signals  
240 that inform decision content inform decision confidence. A different study employing the postdecision wagering paradigm  
241 found that pulvinar neurons represent decision confidence but not perceptual choice<sup>9</sup>. Inactivating the pulvinar altered monkeys  
242 opt-out choice behavior but not their perceptual sensitivity<sup>9</sup>. These results suggest that distinct brain circuits may be responsible  
243 for decision formation and confidence assignment. Consistent with this, studies that employed a post-decision time investment  
244 task found that orbitofrontal cortex neurons in rats play a similar role<sup>12,13</sup> and represent an abstract decision confidence signal<sup>14</sup>.  
245 Our work clarifies how neural circuits can extract such pure decision confidence signals from sensory population activity.  
246 However, note that in some experimental paradigms, the same neurons may represent decision content and confidence<sup>7,10</sup>.

247 We have shown that decoders of V1 activity capture behavioral effects of stimulus manipulations as well as behavioral vari-  
248 ability under repeated presentations of the same stimulus (Fig. 4a,c). Correlations between neural and behavioral  
249 responses can illuminate their causal relationship. However, these correlations can also arise for spurious reasons. Previ-  
250 ous studies employing binary perceptual decision-making tasks found that choice-related signals in sensory cortex reflect a  
251 combination of factors. These include the perceptual decision-making process<sup>36-39</sup>, but also choice-aligned fluctuations in at-  
252 tention<sup>40,41</sup>, expectation<sup>42</sup>, motor planning<sup>43</sup>, and in other unspecified sources that impact sensory activity<sup>44,45</sup>. Could spurious  
253 reasons underlie the association between neural activity and overt behavior in our study? This concern is warranted. There  
254 is no statistical guarantee that the associations we reported primarily reflect the confidence assignment process. However, our  
255 task-design has a unique strength compared to binary decision-making tasks. Subjects generated a two-dimensional choice-  
256 confidence report. Our analysis ensured that both dimensions were orthogonal in neural population space. Nevertheless, we  
257 found that trials that yielded a more extreme perceptual decision variable also resulted in a higher level of confidence (Fig.

258 4e,f). For this association to arise for spurious reasons, there would need to be a factor whose properties are more complex than  
259 simple choice-alignment. It would need to jointly align with perceptual choices and confidence reports. While we cannot rule  
260 out this possibility, we hope that the richness of our behavioral paradigm has helped to expose the confidence computations  
261 implemented by neural circuits downstream of sensory cortex.

262 The ability to recognize which perceptual interpretations of the environment are at risk of being flawed is a hallmark of metacog-  
263 nition and as such often associated with higher intelligence. Our findings suggest that the confidence computations underlying  
264 this ability in the primate brain at least in part arise from simple deterministic transformations of sensory population activity.  
265 These transformations can in principle be realized in basic neural circuits, calling into question the extent to which confidence-  
266 mediated behavior truly provides insight into high level cognitive processes<sup>46</sup>. In general, metacognitive judgements are imper-  
267 fect<sup>24,25,47</sup>. Here, this was evident from the levels of meta-uncertainty displayed by our human and non-human subjects (Fig.  
268 1d). As of yet, we do not know the neural causes of this. Metacognitive inefficiencies may originate in noise in sensory rep-  
269 resentations<sup>29,48-50</sup>. Alternatively, these inefficiencies may arise downstream of sensory cortex, for example from sub-optimal  
270 confidence mapping rules<sup>51</sup>. The task-paradigm and computational framework we have developed offer promising vehicles to  
271 address these outstanding questions and achieve a more complete understanding of the neural mechanisms that underlie and  
272 constrain our sense of confidence.

## 273 METHODS

### 274 Animal subjects

275 Our experiments were performed on two adult male macaque monkeys (*Macaca mulatta*, aged 7 and 10 years old at the time  
276 of the experiments). The animals were trained to perform an orientation discrimination task with saccadic eye movements as  
277 operant responses. Monkey F had previously participated in another research study<sup>22</sup>, Monkey Z had not previously participated  
278 in research studies. All training, surgery, and recording procedures were approved by the University of Texas Institutional  
279 Animal Care and Use Committee and conformed to the National Institutes of Health Guide for the Care and Use of Laboratory  
280 Animals. Under general anesthesia, both animals were implanted with three custom-designed titanium head posts and a titanium  
281 recording chamber which enabled access to V1<sup>52</sup>.

### 282 Apparatus

283 The monkeys were seated in a custom-designed primate chair in front of a gamma-corrected 22-inch CRT monitor (Sony  
284 Trinitron, model GDM-FW900), with their heads restrained using three surgical implants. Stimuli were shown on the CRT  
285 monitor, which was positioned approximately 60 cm away from the monkeys' heads. The CRT had a resolution of 1280 by  
286 1024 pixels with a refresh rate of 75 Hz. Eye position was tracked continuously with an infrared eye tracking system at 1 kHz  
287 (EyeLink 1000, SR Research). Stimuli were presented using the Psychophysics Toolbox<sup>53</sup> in MATLAB (MathWorks). Neural  
288 activity was recorded using the Plexon OmniPlex System (Plexon). Precise temporal registration of task events and neural  
289 activity was obtained through a Datapixx system (Vpixx). All of these systems were integrated using the PLDAPS software  
290 package<sup>54</sup> (<https://github.com/HukLab/PLDAPS>). An analogous setup was used for the human psychophysical experiment,  
291 except that head position was stabilized using a chin rest and the monitor was a Hewlett Packard, model A7217.

### 292 Visual stimuli

293 We constructed oriented visual stimuli by bandpass filtering 3-D luminance noise. The filter was orientation-spatial frequency-  
294 temporal frequency separable. All stimuli were constructed with the same spatial and temporal frequency filter. The filter's  
295 spatial frequency passband was centered at a spatial frequency of 2.5 cycles per degree and had a bandwidth of 0.5 octaves.  
296 Its temporal frequency passband was centered at a speed of 2.5 degrees per second and had a bandwidth of 1 octave. The  
297 filter's orientation bandwidth was 3 degrees. For each stimulus condition, the stimulus set contained five unique filtered noise  
298 movies. Each orientation discrimination experiment included stimuli that varied in orientation and contrast. There was one high  
299 and one low contrast level per experiment. The high contrast value was constant across experiments, the low contrast value  
300 varied somewhat across experiments. The high contrast stimuli spanned a range of 11 different orientations, the number of low  
301 contrast orientations varied across experiments (15 experiments had 11 orientations, 7 had 9, 3 had 7, and 4 had 2).

### 302 Fixation task

303 At the beginning of each recording session, monkeys first performed a passive fixation task. We used a hand-mapping procedure  
304 to estimate the location of the spatial receptive fields of visually responsive units. The average receptive field center estimate  
305 served as the center location for the visual stimuli presented during the rest of the recording session. We conducted an initial  
306 fixation task during which we presented sinusoidal gratings of varying orientation for 1000 ms each. This was followed by the  
307 orientation discrimination task.

### 308 Orientation discrimination task

309 The orientation-discrimination task is a variant of classical visual categorization tasks in which the subject uses a saccadic eye  
310 movement as operant response<sup>42,55,56</sup>. We used a richer version of this task in which subjects are invited to additionally report  
311 their confidence in each perceptual decision. Each trial began when the subject fixated a small white dot at the center of the  
312 screen. Upon fixation, four black choice targets appeared — one in each quadrant of the screen. Targets to the left of the fixation  
313 point represented counter-clockwise decisions, targets to the right clockwise decisions. Upper choice targets indicated high  
314 decision confidence, lower choice targets low confidence. After a variable pre-stimulus fixation period the stimulus appeared in  
315 the near periphery (average eccentricity: monkey F = 4.32°, monkey Z = 3.00°) for 500 ms. Subjects judged the orientation of  
316 the stimulus relative to vertical. The stimulus then disappeared along with the fixation mark and subjects reported their decision  
317 and confidence with a saccadic eye movement to one of the four choice targets. Auditory feedback was given to indicate the  
318 accuracy of the decision and the chosen level of confidence. Specifically, the tone differed for correct and incorrect trials and  
319 the sound was played twice in quick succession for high confidence reports. If the decision was correct, a liquid reward was

320 delivered via a solenoid-operated reward system (New Era). Vertically oriented stimuli received random feedback. Trials in  
321 which the monkey did not saccade to one of the choice targets within 3 seconds were aborted. To incentivize meaningful  
322 confidence reports, there were four possible reward levels. It required one correct decision to move from level 1 to 2, 3 further  
323 correct decisions to move from level 2 to 3, and 3 more to reach level 4. Subjects remained at level 4 until they reported an  
324 incorrect decision with high confidence, which reset the score to level 1. The higher the reward level, the larger the reward for  
325 a correct decision. In addition, correct decisions reported with high confidence were rewarded more generously than correct  
326 decisions reported with low confidence. High confidence rewards for each level were 0.04, 0.16, 0.32, 0.64 ml for monkey F  
327 and 0.116, 0.232, 0.464, 0.928 ml for monkey Z. Low confidence rewards were a scalar function of low confidence reward. This  
328 scalar value varied across sessions and was adjusted to titrate the proportion of high and low confidence responses (average 0.68  
329  $\pm$  0.04 for monkey Z and average 0.82  $\pm$  0.04 for monkey F. Lower scalar values encouraged more high confidence responses  
330 due to a larger reward difference between high and low confidence. Each trial, the current reward level was indicated to the  
331 monkey by the duration of the pre-stimulus fixation period (the lower the reward level, the longer this duration). Both monkeys  
332 managed to stay at the highest reward level for the majority of trials (fraction of trials at reward level 4: monkey F = 64 %,  
333 monkey Z = 80 %). We conducted 12 successful recordings from monkey F and 17 from monkey Z (average number of reward  
334 level 4 trials per session, monkey F = 753; monkey Z = 1026).

### 335 **Human psychophysical experiment**

336 Nineteen human subjects (10 male, 9 female; ages 19-32) with normal or corrected-to-normal vision participated in the exper-  
337 iment. The human behavioral task was the same as the animals' orientation discrimination task, with the exception that the  
338 stimulus was presented more centrally and subjects earned points instead of liquid reward (points per high confidence correct  
339 response as a function of reward level: 2, 4, 8, 16; points per low confidence correct response: 1, 2, 4, 8). Human subjects  
340 began by completing 175 training trials. We used these initial trials to estimate each subject's orientation sensitivity. This  
341 sensitivity estimate determined the range of stimulus orientations used in the main experiment. We chose the range such that  
342 the subjects' overall task performance level would resemble that of the animals. This procedure worked well for all but two  
343 subjects for whom we discarded the first block of trials. Subjects performed the main task in sub-blocks of 50 trials. Subjects  
344 were rewarded with monetary points in the same manner as the macaques were rewarded with liquid reward, and received  
345 analogous auditory feedback at the end of each trial. Every 50 trials, subjects were given additional visual feedback on their  
346 total point count. Subjects completed three blocks of 1100 trials. Eleven subjects judged the same filtered noise stimuli as the  
347 monkeys did, eight subjects were presented with deterministic sinusoidal gratings instead. Because meta-uncertainty did not  
348 systematically differ across both groups of subjects, we included all these datasets in our analysis except for the two subjects  
349 who had poorly calibrated first blocks yielding a total of 17 human observers in this analysis.

### 350 **Behavioral analysis**

351 We measured observers' behavioral capability to discriminate stimulus orientation by fitting the relationship between stimulus  
352 orientation and probability of a 'clockwise' choice with a psychometric function consisting of a lapse rate and a cumulative  
353 Gaussian function. To compare the behavioral capability associated with low and high confidence reports, each psychometric  
354 function had its own steepness parameter (the standard deviation of the cumulative Gaussian). The parameters controlling lapse  
355 rate and the point of subjective equality (the mean of the cumulative Gaussian) were shared across both psychometric functions.  
356 Model parameters were optimized by maximizing the likelihood over observed data, assuming responses arise from a Bernoulli  
357 process. For the analysis documented in Fig. 1c, each dataset was analyzed independently.

358 For each dataset, we obtained an estimate of the subject's level of 'meta-uncertainty' by fitting the CASANDRE model to the  
359 choice-confidence data using a fitting procedure described previously<sup>24</sup>. In brief, the model had eight parameters: the standard  
360 deviation of the decision variable ( $\sigma_d$ ) (one per contrast level, two in total), the decision criterion ( $C_d$ ) (one per contrast level,  
361 two in total), the level of meta-uncertainty ( $\sigma_m$ ), the confidence criterion ( $C_c$ ) (we allowed for choice-dependent asymmetries,  
362 two in total), and lapse rate ( $\lambda$ ). For each dataset, we computed the log-likelihood of a given set of model parameters across all  
363 choice-confidence reports and used an iterative procedure to identify the most likely set of parameter values (specifically, the  
364 interior point algorithm used by the Matlab function 'fmincon'). For the analysis documented in Fig. 1d, the first and last block  
365 of trials completed by the human subjects were analyzed independently.

### 366 **Electrophysiological recordings**

367 During the orientation discrimination task, we recorded extracellular spiking activity from populations of V1 neurons through a  
368 chronically implanted recording chamber. Every recording session, we used a microdrive (Thomas recording) to mechanically  
369 advance one or two linear electrode arrays (Plexon S- and V-probes; 32 or 24 contacts) into the brain. We positioned the linear

arrays so that they roughly spanned the cortical sheet and removed them after each recording session. Continuous neural data were acquired and saved to disk from each channel (sampling rate 30 kHz, Plexon Omniplex System). To extract responses of individual units, we performed offline spike sorting. We first automatically spike-sorted the data with Kilosort<sup>57</sup>, followed by manual merging and splitting as needed (with the ‘phy’ user interface, <https://github.com/kwikteam/phy>). Given that the electrodes’ position could not be optimized for all contact sites, most of our units probably consist of multineuron clusters. We used the fixation task to identify visually responsive units whose activity selectively depended on stimulus orientation. We measured each unit’s response by expressing spike times relative to stimulus onset and counting spikes within a 1,000-ms window following response onset. For each unit, we chose a response latency by maximizing the stimulus-associated response variance<sup>58</sup>. We visually inspected orientation tuning curves and excluded untuned units from further analysis.

## 379 Linear decoders

To assess how well the recorded populations could support the perceptual task, we trained linear *stimulus decoders* to discriminate between clockwise and counterclockwise stimuli. We used all stimuli whose orientation differed from 0 degrees. We first Z-scored each unit’s spike counts. We then used these z-scored responses to estimate the set of linear weights,  $\mathbf{w} = (w_1, \dots, w_n)$  that best separate clockwise and counter-clockwise stimulus response patterns, assuming a multivariate Gaussian response distribution:

$$\mathbf{w} = \frac{s}{\Sigma} \quad (1)$$

380 Where  $s$  is the mean difference of the stimulus-category conditioned Z-scored responses and  $\Sigma$  is the covariance matrix of  
381 the Z-scored responses. The decoder weights are calculated from observed trials. To avoid double-dipping, we excluded the  
382 trial under consideration from the calculation and solely used all other trials to estimate the weights. This way, we obtained a  
383 ‘cross-validated’ stimulus judgement from the linear stimulus decoder for each trial. We quantified how well these decoders  
384 captured the animals’ behavior by computing the fraction of consistent perceptual choices and subtracting the number expected  
385 by chance based on the decoder’s and the animal’s overall success rate (Fig. 2b). In a later analysis, we compared nonlinear  
386 *choice* and *confidence decoders* with their linear counterparts (Fig. 2e,f). For this analysis, we used exactly the same set of  
387 training and hold-out trials for the linear decoders as we used for the nonlinear decoders.

## 388 Nonlinear decoders

389 We trained feed-forward multi-layer perceptron neural networks on Z-scored V1 responses to either predict the animals’ per-  
390 ceptual choice or their confidence report. We implemented networks within the TensorFlow framework using the AdamW  
391 optimiser with an objective to minimize binary cross-entropy. Models consisted of 1 hidden layer with 15 hidden units per  
392 layer, had a dropout rate between layers of 0.1, and the learning rate was set to 0.001. We explored various hyper-parameter set-  
393 tings and found the results presented here to be robust across settings. We trained networks on 80% of trials (training/validation  
394 set) and obtained a cross-validated prediction on the held out 20% of trials, rotating trials between training and held out set  
395 such that each trial had a cross-validated prediction (Fig. 2e,f). To ensure that every trial would be part of the hold out set, we  
396 trained 30 different networks per dataset. Just like we did for the linear decoders, we solely used cross-validated choice and  
397 confidence predictions in our analysis. For each trial, we selected the decoder’s prediction from the “first” network in which  
398 this trial was held out. We found 30 networks to be sufficient for every trial to be held out at least once.

399 We ensured that choice decoders could not use decision confidence to predict choices and that confidence decoders could not  
400 use perceptual choice to predict confidence. Specifically, we orthogonalized choice and confidence information in the training  
401 trials by maintaining a fixed ratio of high and low confidence reports across clockwise and counterclockwise choices and a  
402 fixed ratio of clockwise and counterclockwise choices across high and low confidence reports. To do so, we randomly selected  
403 trials from under-represented trial types (e.g “high-confident counter-clockwise”) and concatenated them to the training set.  
404 To minimize potentially confounding influences of cross-trial variation in the animals’ motivation, attention, and alertness, we  
405 only included “reward level 4” trials in the training set. Training sets on average contained 1088 trials.

406 To interrogate whether the confidence decoders extracted meaningful information from V1 responses, we compared the slope  
407 of the psychometric function conditioned on the confidence decoder’s output (Fig. 3a). This comparison is most reliable when  
408 both psychometric functions contain a similar number of trials. We achieved this by using the median of the latent confidence  
409 variable as confidence criterion. We did this for both high and low contrast trials.

410 We probed the confidence decoders with synthetic patterns of neural activity (Fig. 3c). To create these patterns, we first  
411 computed the cross-trial average firing rate per unit for a given stimulus orientation using only high contrast, reward level 4  
412 trials. We manipulated the gain of these responses by multiplying this average population response with a scalar factor. For  
413 each recording session, we randomly picked on the 30 trained networks for this analysis (Fig. 3d).

414 We studied the decoders' latent variables (Fig. 4). This analysis involved computing a discriminability index. To do so, we  
 415 first Z-scored the latent variables per stimulus condition, thus removing stimulus-driven effects. We then created two groups  
 416 of trials based on the animals' behavioral reports (either their perceptual choice or their confidence report). We included all  
 417 stimulus conditions for which both response options had been used at least 5 times. Finally, we computed the area under the  
 418 curve for both sets of trials<sup>36</sup>.  
 419

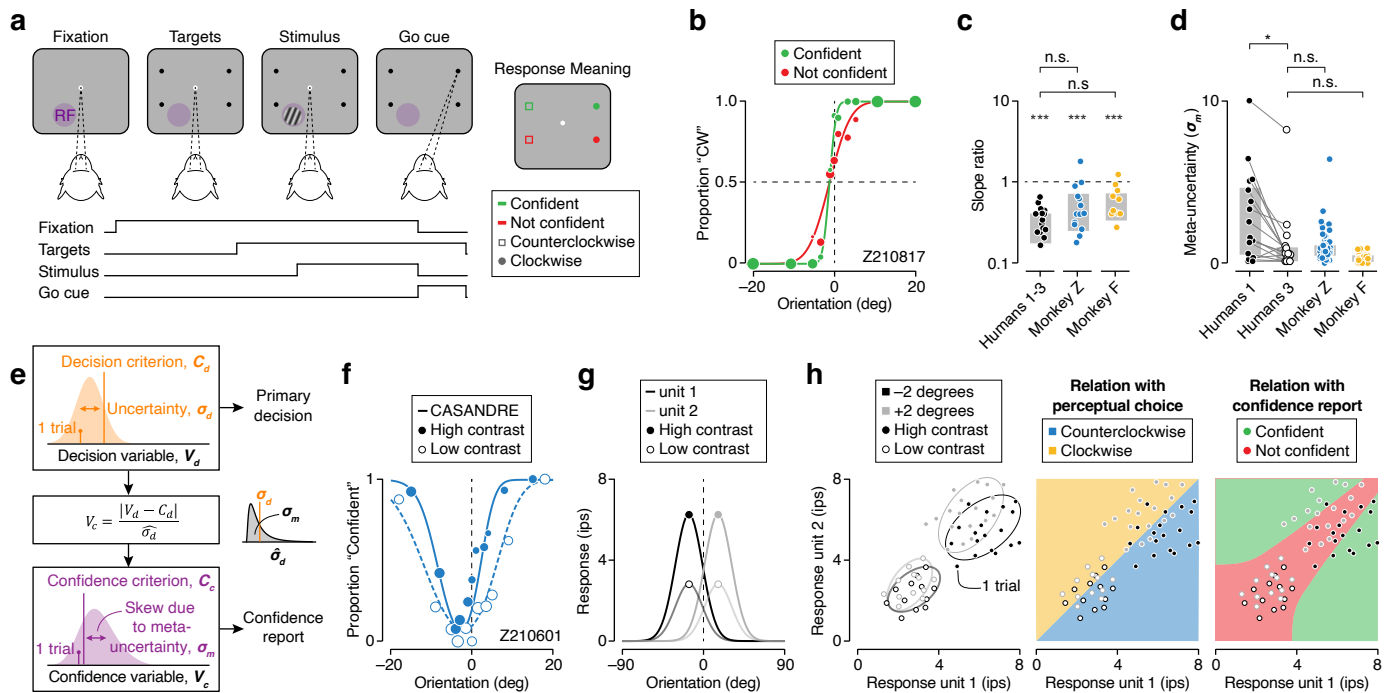


**Figure 1** Perceptual confidence task: behavior and computational hypothesis. **(a)** Orientation discrimination task sequence. After the observer fixates for at least 500 ms, four choice targets appear, followed by the stimulus. The stimulus is placed in the neurons' visual receptive field (RF). The observer judges whether the stimulus is rotated clockwise or counterclockwise relative to vertical. They jointly communicate this orientation judgment and their decision confidence with a saccade towards one of four choice targets. Horizontal saccade direction indicates the perceptual judgment, vertical saccade direction the confidence report. Correct decisions are followed by a juice reward (Methods). **(b)** Psychophysical performance for monkey Z in an example recording session. Proportion of clockwise (CW) choices for high-contrast stimuli is shown as a function of stimulus orientation, conditioned on the observer's confidence report. Symbol size reflects the number of trials (total 527 trials, slope ratio = 0.57). The curves are fits of a behavioral model (Methods). **(c)** The ratio of the slope of high contrast psychometric functions. Sensible confidence judgments yield values smaller than one. Grey bars indicate interquartile range. **(d)** Meta-uncertainty for a group of human subjects and two monkeys. For the humans, each symbol represents metacognitive performance of one subject in one block of trials. For the monkeys, each symbol represent metacognitive performance in one behavioral session (humans: n = 17; monkey Z: n = 60; monkey F: n = 58). Grey bars indicate interquartile range. **(e)** Schematic of a process model for decision confidence<sup>24</sup>. **(f)** Proportion high confidence judgments as a function of stimulus orientation for high and low contrast stimuli (filled vs open symbols) in an example recording session. Symbol size reflects the number of trials (total 744 trials). Solid lines are fits of the process model shown in panel **e**. **(g)** Average firing rate as a function of stimulus orientation for two model neurons (black vs grey) and two stimulus contrasts (open vs closed symbols). **(h)** (Left) Joint responses of a pair of model neurons to repeated presentations of four stimuli that differ in orientation and contrast. (Middle) Illustration of a mapping rule that converts the pairwise activity into a perceptual decision. (Right) Illustration of a mapping rule that converts the same responses into a confidence report. Decision confidence is high when the sensory response is strong (towards upper right corner) and non-ambiguous (away from line of unity). n.s. not significant, \* P < 0.05, \*\* P < 0.01, \*\*\* P < 0.001.

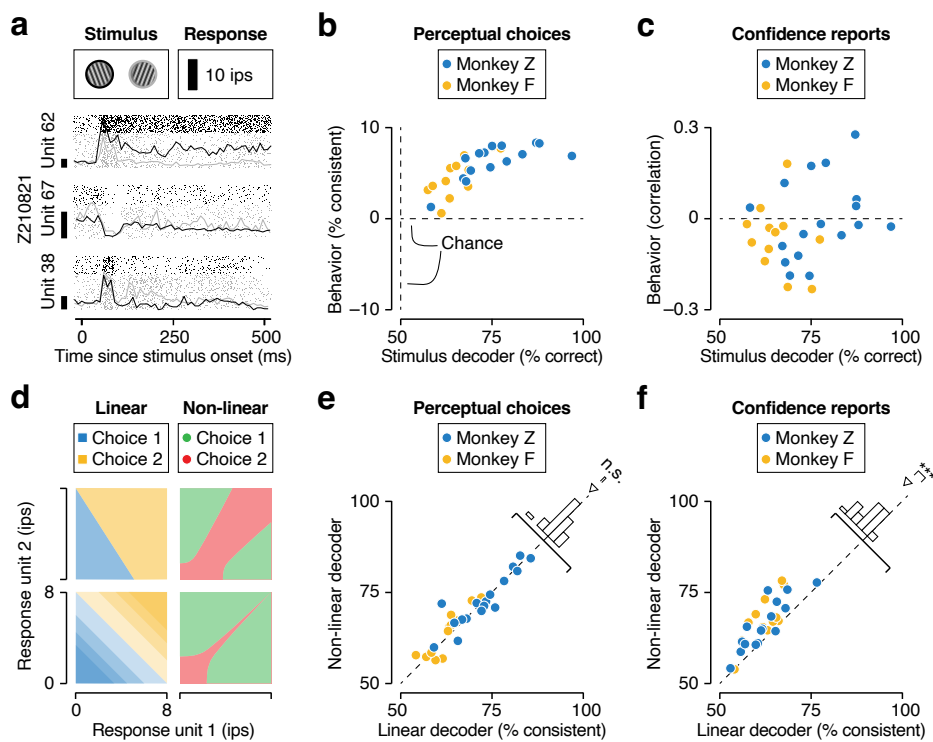


**Figure 2** Predicting perceptual decisions and decision confidence from V1 population activity. **(a)** Spike rasters (dots) and PSTHs (lines) of three example units during presentation of a clockwise (gray) and counterclockwise (black) stimulus. **(b)** Analysis of the linear stimulus decoder. The proportion of correctly predicted perceptual choices minus the proportion expected by chance is plotted against the decoder's task performance. Each symbol represents a recording session. **(c)** The correlation between the monkeys' confidence reports and the linear stimulus decoder's output is plotted against the decoder's task performance. **(d)** Example mapping rules that can be implemented by a linear (left) and non-linear (right) decoder. **(e)** Comparison of the proportion correctly predicted perceptual choices by a linear (abscissa) and non-linear (ordinate) choice decoder. **(f)** Comparison of the proportion correctly predicted confidence reports by a linear (abscissa) and non-linear (ordinate) confidence decoder. n.s. not significant, \*  $P < 0.05$ , \*\*  $P < 0.01$ , \*\*\*  $P < 0.001$ .

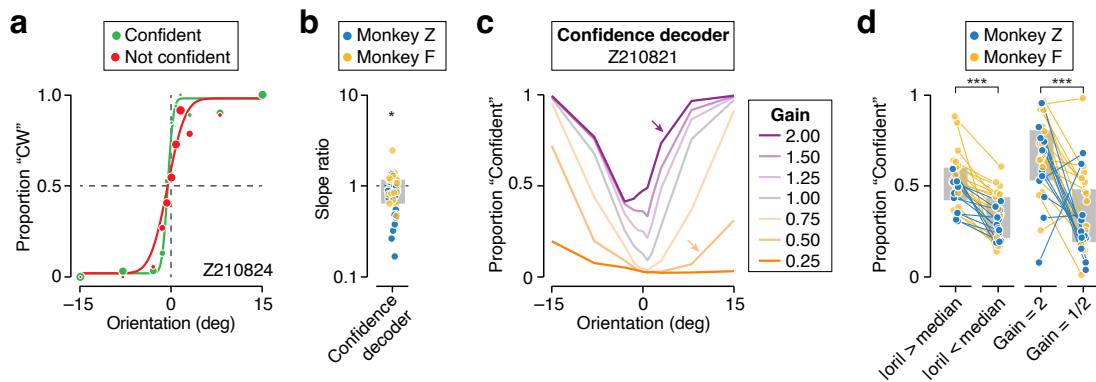


**Figure 3** The non-linear confidence decoder yields sensible and robust outputs. **(a)** Psychophysical performance for monkey Z in an example recording session. Proportion of clockwise (CW) choices for high-contrast stimuli is shown as a function of stimulus orientation, conditioned on the confidence decoder's output. Symbol size reflects the number of trials (total 520 trials, slope ratio = 0.88). The curves are fits of a behavioral model. **(b)** The ratio of the slope of both psychometric functions. Grey bars indicate interquartile range. **(c)** Illustration of the confidence decoder's output for various synthetic patterns of neural activity for an example recording session. **(d)** Summary of the synthetic confidence experiments for all recording sessions. (Left) Proportion of predicted high confidence outputs elicited by stimuli whose orientation is more or less extreme than the median stimulus orientation. (Right) Proportion of high confidence outputs elicited by sensory input patterns with a high or low response gain (indicated by the colored arrows in panel c). Grey bars indicate interquartile range. n.s. not significant, \*  $P < 0.05$ , \*\*  $P < 0.01$ , \*\*\*  $P < 0.001$ .

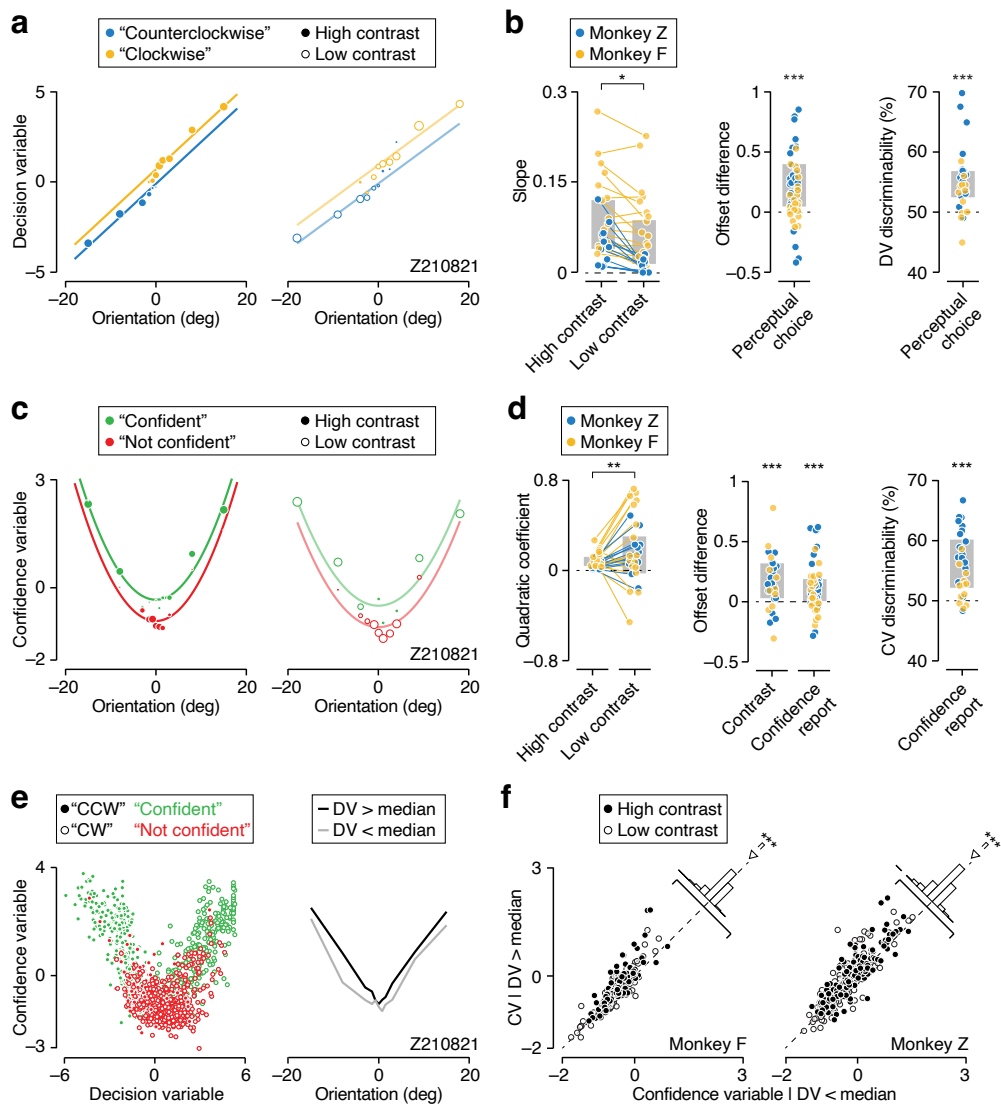


**Figure 4** The decoders' latent variables follow the predictions of a computational framework of perceptual decision confidence. (a) The latent variable of the nonlinear choice decoder plotted against stimulus orientation, for high and low contrast trials (left vs right), conditioned on the animal's perceptual choice (yellow vs blue) for an example dataset. (b) Summary of the decision variable's statistical structure across all recording sessions. Grey bars indicate interquartile range. (c) The latent variable of the nonlinear confidence decoder plotted against stimulus orientation, for high and low contrast trials (left vs right), conditioned on the animal's confidence report (red vs green) for an example dataset. (d) Summary of the confidence variable's statistical structure across all recording sessions. Grey bars indicate interquartile range. (e) Direct comparison of the confidence variable and the decision variable. (Left) Each point represents a single trial in an example recording session. (Right) The mean confidence level plotted against stimulus orientation for trials with a decision variable value that is more (black) or less (gray) extreme than the stimulus-specific median. (f) Summary of the median-split analysis illustrated in panel e for all recording sessions. Each data point represents a single stimulus condition. n.s. not significant, \*  $P < 0.05$ , \*\*  $P < 0.01$ , \*\*\*  $P < 0.001$ .

## 420 References

1. S. Hecht, S. Shlaer, and M. H. Pirenne. Energy, quanta, and vision. *Journal of General Physiology*, 25:819–840, 1942.
2. Wilson P. Tanner Jr. and John A. Swets. A decision-making theory of visual detection. *Psychological Review*, 61(6):401–409, 1954.
3. David Marvin Green and John A. Swets. *Signal detection theory and psychophysics*, volume 1. Wiley New York, 1966.
4. L. Festinger. Studies in decision: I. Decision-time, relative frequency of judgment and subjective confidence as related to physical stimulus difference. *Journal of Experimental Psychology*, 32(4):291–306, 1943.
5. Pascal Mamassian. Visual Confidence. *Annual Review of Vision Science*, 2(1):459–481, 2016.
6. A. Pouget, J. Drugowitsch, and A. Kepcs. Confidence and certainty: distinct probabilistic quantities for different goals. *Nature neuroscience*, 19(3):366–374, 2016.
7. Roozbeh Kiani and Michael N. Shadlen. Representation of confidence associated with a decision by neurons in the parietal cortex. *Science*, 324(5928):759–764, 2009.
8. Paul Middlebrooks and Marc Sommer. Metacognition in monkeys during an oculomotor task. *Journal of experimental psychology. Learning, memory, and cognition*, 37(2):325–337, March 2011.
9. Yutaka Komura, Akihiko Nikkuni, Noriko Hirashima, Teppei Uetake, and Aki Miyamoto. Responses of pulvinar neurons reflect a subject's confidence in visual categorization. *Nature Neuroscience*, 16(6):749–755, June 2013.
10. Christopher R. Fetsch, Roozbeh Kiani, William T. Newsome, and Michael N. Shadlen. Effects of cortical microstimulation on confidence in a perceptual decision. *Neuron*, 83(4):797–804, 2014.
11. Brian Odegaard, Piercesare Grimaldi, Seong Hah Cho, Megan A. K. Peters, Hakwan Lau, and Michele A. Basso. Superior colliculus neuronal ensemble activity signals optimal rather than subjective confidence. *Proceedings of the National Academy of Sciences*, 115(7):E1588–E1597, February 2018.
12. Adam Kepcs, Naoshige Uchida, Hatim A. Zariwala, and Zachary F. Mainen. Neural correlates, computation and behavioural impact of decision confidence. *Nature*, 455(7210):227–231, September 2008.
13. Armin Lak, Gil M. Costa, Erin Romberg, Alexei A. Koulakov, Zachary F. Mainen, and Adam Kepcs. Orbitofrontal Cortex Is Required for Optimal Waiting Based on Decision Confidence. *Neuron*, 84(1):190–201, October 2014.
14. Paul Masset, Torben Ott, Armin Lak, Junya Hirokawa, and Adam Kepcs. Behavior- and Modality-General Representation of Confidence in Orbitofrontal Cortex. *Cell*, 182(1):112–126.e18, July 2020.
15. Braden A. Purcell and Roozbeh Kiani. Hierarchical decision processes that operate over distinct timescales underlie choice and changes in strategy. *Proceedings of the National Academy of Sciences*, 113(31):E4531–E4540, August 2016.
16. Jan Drugowitsch, André G. Mendonça, Zachary F. Mainen, and Alexandre Pouget. Learning optimal decisions with confidence. *Proceedings of the National Academy of Sciences*, 116(49):24872–24880, December 2019.
17. Morteza Sarafyazd and Mehrdad Jazayeri. Hierarchical reasoning by neural circuits in the frontal cortex. *Science*, 364(6441):eaav8911, May 2019.
18. Bahador Bahrami, Karsten Olsen, Peter E. Latham, Andreas Roepstorff, Geraint Rees, and Chris D. Frith. Optimally interacting minds. *Science*, 329(5995):1081–1085, August 2010.
19. N. K. Logothetis and J. D. Schall. Neuronal correlates of subjective visual perception. *Science*, 245(4919):761–763, August 1989.
20. M. N. Shadlen and W. T. Newsome. Neural basis of a perceptual decision in the parietal cortex (area LIP) of the rhesus monkey. *Journal of Neurophysiology*, 86(4):1916–1936, October 2001.
21. Joshua I. Gold and Michael N. Shadlen. The neural basis of decision making. *Annual Review of Neuroscience*, 30:535–574, 2007.
22. Julie A. Charlton and Robbe L. T. Goris. Abstract deliberation by visuomotor neurons in prefrontal cortex. *Nature Neuroscience*, pages 1–9, April 2024.
23. D. H. Hubel and T. N. Wiesel. Receptive fields and functional architecture of monkey striate cortex. *The Journal of Physiology*, 195(1):215–243, March 1968.
24. Zoe M. Boundy-Singer, Corey M. Ziembka, and Robbe L. T. Goris. Confidence reflects a noisy decision reliability estimate. *Nature Human Behaviour*, 7(1):142–154, January 2023.
25. Medha Shekhar and Dobromir Rahnev. The nature of metacognitive inefficiency in perceptual decision making. *Psychological Review*, 128(1):45–70, 2021.
26. Pascal Mamassian and Vincent de Gardelle. Modeling perceptual confidence and the confidence forced-choice paradigm. *Psychological Review*, 129(5):976–998, October 2022.
27. Baptiste Caziot and Pascal Mamassian. Perceptual confidence judgments reflect self-consistency. *Journal of Vision*, 21(12):8, November 2021.
28. Gergő Orban, Pietro Berkes, József Fiser, and Máté Lengyel. Neural variability and sampling-based probabilistic representations in the visual cortex. *Neuron*, 92(2):530–543, 2016.
29. Olivier J. Henaff, Zoe M. Boundy-Singer, Kristof Meding, Corey M. Ziembka, and Robbe L. T. Goris. Representation of visual uncertainty through neural gain variability. *Nature Communications*, 11(1):2513, May 2020.
30. Dylan Festa, Amir Aschner, Aida Davila, Adam Kohn, and Ruben Coen-Cagli. Neuronal variability reflects probabilistic inference tuned to natural image statistics. *Nature Communications*, 12(1):3635, June 2021.
31. Robbe L. T. Goris, Ruben Coen-Cagli, Kenneth D. Miller, Nicholas J. Priebe, and Máté Lengyel. Response sub-additivity

480 and variability quenching in visual cortex. *Nature Reviews Neuroscience*, 25(4):237–252, April 2024.

481 32. Robert Geirhos, Jörn-Henrik Jacobsen, Claudio Michaelis, Richard Zemel, Wieland Brendel, Matthias Bethge, and Felix A.  
482 Wichmann. Shortcut learning in deep neural networks. *Nature Machine Intelligence*, 2(11):665–673, November 2020.

483 33. B. C. Skottun, A. Bradley, G. Sclar, I. Ohzawa, and R. D. Freeman. The effects of contrast on visual orientation and spatial  
484 frequency discrimination: a comparison of single cells and behavior. *Journal of Neurophysiology*, 57(3):773–786, March  
485 1987.

486 34. D. J. Heeger. Normalization of cell responses in cat striate cortex. *Visual Neuroscience*, 9(2):181–197, August 1992.

487 35. David Ferster and Kenneth D. Miller. Neural mechanisms of orientation selectivity in the visual cortex. *Annual review of  
488 neuroscience*, 23(1):441–471, 2000.

489 36. K. H. Britten, W. T. Newsome, M. N. Shadlen, S. Celebrini, and J. A. Movshon. A relationship between behavioral choice  
490 and the visual responses of neurons in macaque MT. *Visual Neuroscience*, 13(1):87–100, February 1996.

491 37. J. V. Dodd, K. Krug, B. G. Cumming, and A. J. Parker. Perceptually bistable three-dimensional figures evoke high choice  
492 probabilities in cortical area MT. *The Journal of Neuroscience: The Official Journal of the Society for Neuroscience*,  
493 21(13):4809–4821, July 2001.

494 38. Adrian G. Bondy, Ralf M. Haefner, and Bruce G. Cumming. Feedback determines the structure of correlated variability in  
495 primary visual cortex. *Nature Neuroscience*, 21(4):598–606, April 2018.

496 39. Ralf M. Haefner, Pietro Berkes, and József Fiser. Perceptual Decision-Making as Probabilistic Inference by Neural Sampling.  
497 *Neuron*, 0(0), April 2016.

498 40. Hendrikje Nienborg and Bruce G. Cumming. Decision-related activity in sensory neurons reflects more than a neuron's  
499 causal effect. *Nature*, 459(7243):89–92, May 2009.

500 41. Katrina R. Quinn, Lenka Seillier, Daniel A. Butts, and Hendrikje Nienborg. Decision-related feedback in visual cortex lacks  
501 spatial selectivity. *Nature Communications*, 12(1):4473, July 2021.

502 42. Robbe L. T. Goris, Corey M. Ziembra, Gabriel M. Stine, Eero P. Simoncelli, and J. Anthony Movshon. Dissociation of Choice  
503 Formation and Choice-Correlated Activity in Macaque Visual Cortex. *Journal of Neuroscience*, 37(20):5195–5203, May  
504 2017.

505 43. Pooya Laamerad, Liu D. Liu, and Christopher C. Pack. Decision-related activity and movement selection in primate visual  
506 cortex. *Science Advances*, 10(22):eadk7214, May 2024.

507 44. Aaron J. Levi, Yuan Zhao, Il Memming Park, and Alexander C. Huk. Sensory and Choice Responses in MT Distinct from  
508 Motion Encoding. *Journal of Neuroscience*, 43(12):2090–2103, March 2023.

509 45. Corey M. Ziembra, Robbe L. T. Goris, Gabriel M. Stine, Richard K. Perez, Eero P. Simoncelli, and J. Anthony Movshon.  
510 Neuronal and behavioral responses to naturalistic texture images in macaque monkeys, February 2024. Available from  
511 <http://doi.org/10.1101/2024.02.22.581645>.

512 46. Navindra Persaud, Peter McLeod, and Alan Cowey. Post-decision wagering objectively measures awareness. *Nature  
513 Neuroscience*, 10(2):257–261, February 2007.

514 47. Thomas O. Nelson. A comparison of current measures of the accuracy of feeling-of-knowing predictions. *Psychological  
515 Bulletin*, 95(1):109–133, 1984.

516 48. P. Heggelund and K. Albus. Response variability and orientation discrimination of single cells in striate cortex of cat. *Experimental  
517 Brain Research*, 32(2):197–211, June 1978.

518 49. Robbe L. T. Goris, J. Anthony Movshon, and Eero P. Simoncelli. Partitioning neuronal variability. *Nature Neuroscience*,  
519 17(6):858–865, June 2014.

520 50. Zoe M. Boundy-Singer, Corey M. Ziembra, Olivier J. Hénaff, and Robbe L. T. Goris. How does V1 population activity inform  
521 perceptual certainty?, September 2023. Available from <http://doi.org/10.1101/2023.09.08.556926>.

522 51. Jeffrey M. Beck, Wei Ji Ma, Xaq Pitkow, Peter E. Latham, and Alexandre Pouget. Not Noisy, Just Wrong: The Role of  
523 Suboptimal Inference in Behavioral Variability. *Neuron*, 74(1):30–39, April 2012.

524 52. Daniel L. Adams, John R. Economides, Cristina M. Jocson, John M. Parker, and Jonathan C. Horton. A watertight acrylic-  
525 free titanium recording chamber for electrophysiology in behaving monkeys. *Journal of Neurophysiology*, 106(3):1581–1590,  
526 September 2011.

527 53. D. H. Brainard. The Psychophysics Toolbox. *Spatial Vision*, 10(4):433–436, 1997.

528 54. Kyler Eastman and Alexander Huk. PLDAPS: A Hardware Architecture and Software Toolbox for Neurophysiology Requiring  
529 Complex Visual Stimuli and Online Behavioral Control. *Frontiers in Neuroinformatics*, 6, 2012.

530 55. William T. Newsome, Kenneth H. Britten, and J. Anthony Movshon. Neuronal correlates of a perceptual decision. *Nature*,  
531 341(6237):52–54, September 1989.

532 56. Hendrikje Nienborg and Bruce G. Cumming. Decision-Related Activity in Sensory Neurons May Depend on the Columnar  
533 Architecture of Cerebral Cortex. *Journal of Neuroscience*, 34(10):3579–3585, 2014.

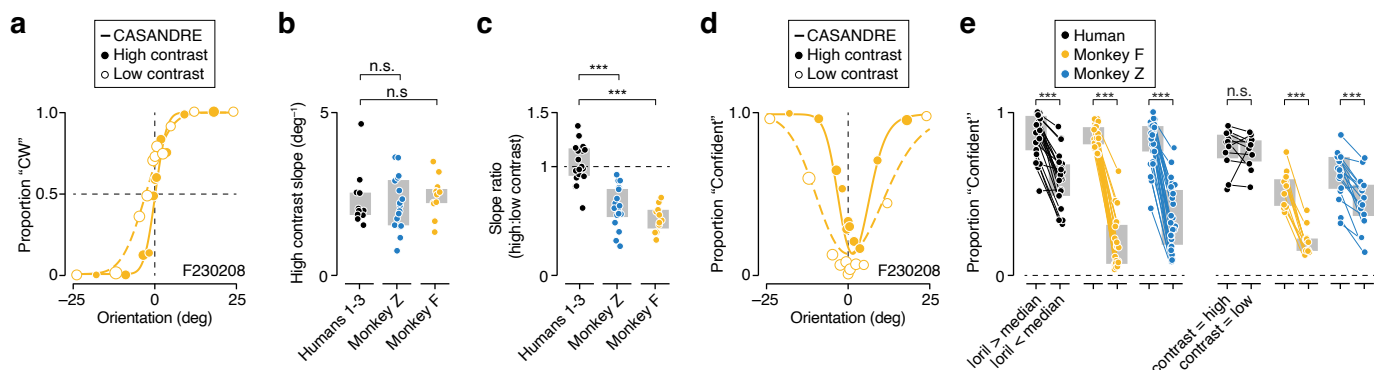
534 57. Marius Pachitariu, Nicholas A Steinmetz, Shabnam N Kadir, Matteo Carandini, and Kenneth D Harris. Fast and accurate  
535 spike sorting of high-channel count probes with KiloSort. In *Advances in Neural Information Processing Systems*, volume 29.  
536 Curran Associates, Inc., 2016.

537 58. Matthew A. Smith, Najib J. Majaj, and J. Anthony Movshon. Dynamics of motion signaling by neurons in macaque area MT.  
538 *Nature Neuroscience*, 8(2):220–228, February 2005.

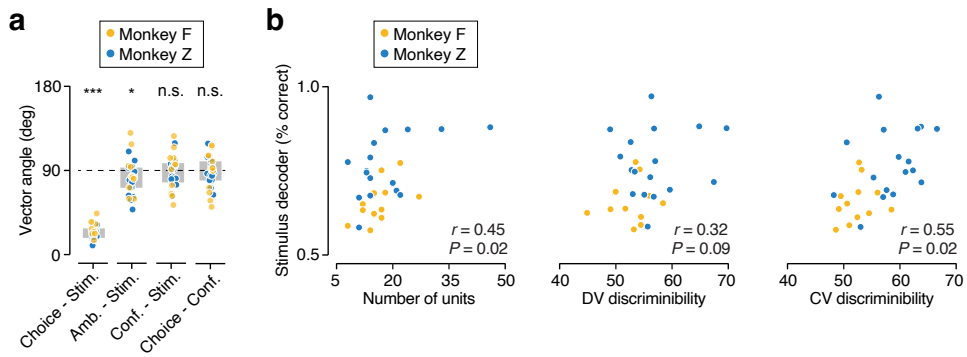


541

## Supplementary Information



**Supplementary Figure 1** Further comparison of human and monkey behaviour. (a) Psychophysical performance for monkey F in an example recording session. Proportion of clockwise (CW) choices is shown as a function of stimulus orientation for high and low contrast stimuli (filled vs open symbols). Symbol size reflects the number of trials (total 1390 trials, slope ratio = 0.46). The curves are fits of a process model for confidence (CASANDRE<sup>24</sup>). (b) Analysis of perceptual sensitivity. The slope of the high contrast psychometric function is shown for a group of human observers and both monkeys. We only included the human subjects for whom stimulus contrast and stochasticity was identical to the values used in the monkey experiments ( $n = 11$ ). Orientation sensitivity of the humans and monkeys was comparable. Grey bars indicate interquartile range. (c) The ratio of the slope of the high and low contrast psychometric functions for a group of human subjects and both monkeys. The contrast manipulation had a stronger impact on the monkeys' perceptual sensitivity. We speculate that this may be due to the stimuli being presented more centrally in the human experiments. Grey bars indicate interquartile range. (d) Proportion of high confidence judgments as a function of stimulus orientation for high and low contrast stimuli (filled vs open symbols) in an example recording session. (e) (Left) Proportion of high confidence reports elicited by stimuli whose orientation is more or less extreme than the median stimulus orientation. (Right) Proportion of high confidence reports elicited by high and low contrast stimuli. Grey bars indicate interquartile range. n.s. not significant, \*  $P < 0.05$ , \*\*  $P < 0.01$ , \*\*\*  $P < 0.001$ .



**Supplementary Figure 2** Further analysis of linear and non-linear decoders. **(a)** Comparison of the orientation of the hyperplanes used to slice neural population space by a linear *choice* decoder (trained on all data), *stimulus* decoder (trained on all non-ambiguous trials), *ambiguous* decoder (trained to predict choices on ambiguous trials only), and *confidence* decoder (trained on all data). Unrelated hyperplanes tend to be orthogonal in high-dimensional spaces (vector angle = 90 deg). Note that this is not the case for the choice and stimulus decoder, nor for the stimulus and ambiguous decoder. Grey bars indicate interquartile range. **(b)** Task performance of the linear stimulus decoder is plotted against the number of units in the population (left), the non-linear choice decoder's latent variable's discriminability (middle), and the non-linear confidence decoder's latent variable's discriminability (right). Larger neural populations tended to be better able to support the perceptual task. Populations that contained more stimulus information tended to enable better decoding of perceptual choices and confidence reports. n.s. not significant, \*  $P < 0.05$ , \*\*  $P < 0.01$ , \*\*\*  $P < 0.001$ .